JACS
JOURNAL OF THE AMERICAN CHEMICAL SOCIETY

COMMUNICATION

pubs.acs.org/JACS

Multilayer Assembly of Nanowire Arrays for Dye-Sensitized Solar Cells

Chengkun Xu, Jiamin Wu, Umang V. Desai, and Di Gao*

Department of Chemical and Petroleum Engineering, University of Pittsburgh, Pittsburgh, Pennsylvania 15261, United States

Supporting Information

ABSTRACT: Vertically ordered nanostructures synthesized directly on transparent conducting oxide have shown great promise for overcoming the limitations of current dye-sensitized solar cells (DSCs) based on random networks of nanoparticles. However, the synthesis of such structures with a high internal surface area has been challenging. Here we demonstrate a convenient approach that involves alternate cycles of nanowire growth and self-assembled monolayer coating processes for synthesizing multilayer assemblies of ZnO nanowire arrays and using the assemblies for fabrication of DSCs. The assembled multilayer ZnO nanowire arrays possess an internal surface area that is more than 5 times larger than what one can possibly obtain with single-layer nanowire arrays. DSCs fabricated using such multilayer arrays yield a power conversion efficiency of 7%, which is comparable to that of TiO_2 nanoparticle-based DSCs. The ordered structure with a high internal surface area opens up opportunities for further improvement of DSCs.

Dye-sensitized solar cells (DSCs) are among the most promising devices for low-cost solar-to-electricity energy conversion. Although an energy conversion efficiency of 11% has been demonstrated for such cells, researchers are still seeking to increase the efficiency further by using alternative sensitizers[1,2] and redox electrolytes[3,4] and to fabricate solid-state or nonvolatile-liquid DSCs.[5,6] The progress of these efforts, however, has been impeded by the disordered structure of mesoporous TiO_2 films used in current DSCs. The mesoporous TiO_2 films, which are composed of sintered TiO_2 nanoparticles, induce a short electron diffusion length (10−35 μm,[7] as determined by the product of the electron diffusion coefficient and electron lifetime) that limits further improvement in DSC performance.[8,9] The disordered porous structure also makes infiltration of solid or viscous electrolytes into the electrodes difficult and ineffective.[10,11] The synthesis and fabrication of vertically aligned 1D nanostructures directly on transparent conducting oxides (TCOs) has been identified as a promising means of overcoming these issues.[8,12] Recent studies have shown that photoanodes based on ordered 1D arrays lead to a significantly increased electron diffusion length on the order of 100 μm.[13−16] This should allow improvement of the energy conversion efficiency by increasing the thickness of the sensitized films or using kinetically faster redox couples. The vertically ordered structure should also facilitate the filling of solid-state electrolyte or ionic liquid into the sensitized films.

One key challenge of using vertically aligned 1D nanostructures in DSCs is that in comparison with mesoporous films, the 1D nanostructures typically have a low internal surface area, resulting in insufficient dye adsorption and therefore low light-harvesting efficiency.[17−20] As a result, the efficiency of DSCs based on vertically aligned 1D nanostructures is significantly lower than that of nanoparticle-based ones. Although an efficiency of 6.9%, currently the highest value reported for DSCs of this kind, was recently achieved[21] using TiO_2 nanotube arrays fabricated on TCO, the fabrication process involved complex sputtering and anodization of thick Ti films, which are difficult to scale up both technically and economically. Therefore, fabrication of arrays of long, vertically aligned 1D nanostructures by an economically viable method remains challenging. In our previous work,[22] we developed a wet chemical process for rapid growth of ZnO nanowire arrays. With this process, ZnO nanowires with lengths of >40 μm long can be readily obtained. However, such long wires are typically fused at their roots, and as a result, a significant percentage of the surface area gained by increasing the wire length is lost. Fusion of the wires, which is largely due to the widening of the wires as they grow long, occurs in almost all of the published methods for growing ZnO nanowires in chemical baths. Therefore, to avoid wire fusion, a method for growing wires only at the top surface while protecting the lower section of the wires is needed. Here we present an innovative solution to this challenge based on the synthesis of multilayer assemblies of ZnO nanowire arrays, which possess an internal surface area that is >5 times larger than that of single-layer ZnO nanowire arrays.

In our process, a key strategy for preventing the fusion of wires at their roots is growing the wires in multiple stages: wires grow only ∼10 μm in each stage, and a self-assembled monolayer (SAM) coating is used to protect the wires grown in previous stages from widening and fusing in the next growth stage. This process is shown schematically in Figure 1 and can be described as follows. First, we grow one layer of ZnO nanowires directly on TCO (Figure 1a). Through the wet chemical process previously developed by our group,[22] vertically aligned ZnO nanowires up to 10 μm long can be obtained easily without fusion of the roots of the wires. Second, we coat the surface of the first-layer wires with a SAM coating formed from the precursor octadecyltrichlorosilane, $CH_3(CH_2)_{17}SiCl_3$ (OTS) (Figure 1b). Prior to the growth of the second-layer wires, the SAM coating at the top end of the first-layer wires is removed by ultraviolet ozone (UVO) treatment while the coating on the side walls of the wires is left (Figure 1c). The SAM coating on the side walls of the ZnO nanowires prevents the aqueous solution from entering the gaps between the wires when the substrate is placed into the chemical bath for growth of the second-layer nanowires, and the aqueous solution comes into contact with the wires only at their top ends. Thus, the wires of the second layer grow only on top of the first layer, and the first-layer wires are not widened (Figure 1d). This process may be repeated multiple times to obtain a multilayer assembly of nanowire arrays until a desired total length for the wires or a desired internal surface area for the entire multilayer assembly is

Received: March 8, 2011
Published: April 28, 2011

ACS Publications © 2011 American Chemical Society

dx.doi.org/10.1021/ja202135n | J. Am. Chem. Soc. 2011, 133, 8122–8125

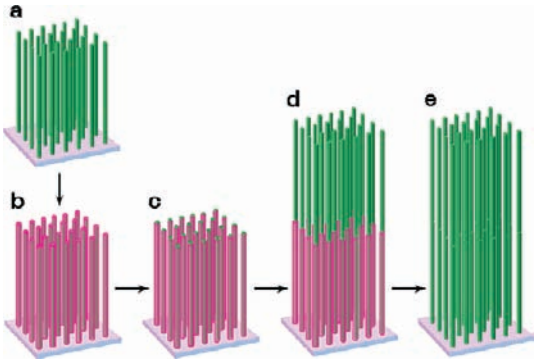

Figure 1. Schematic process for synthesizing a two-layer assembly of ZnO nanowire arrays on TCO. (a) Growth of the first-layer ZnO nanowire array on seeded TCO. (b) Coating of the ZnO nanowire array with SAMs. (c) Selective removal of the SAM coating at the top end of the wires while leaving the SAMs on the side walls of the wires. (d) Growth of the second-layer ZnO nanowire array using the top ends of the first-layer wires as seeds. The aqueous solution comes into contact with only the top ends of the first-layer wires and cannot enter the gaps between the wires because of the SAMs on their side walls. (e) Removal of the SAMs from the side walls of the wires by calcination.

reached. Finally, the SAM coating can be removed by calcination (Figure 1e) before subsequent DSC fabrication steps.

Figure 2a shows a scanning electron microscopy (SEM) image of the first-layer ZnO nanowire array grown directly on TCO. The ZnO nanowires are ~10 μm long and 200 nm wide. It should be noted that in order to reduce the possibility of wires fusing at their roots, the concentration of the $Zn(NO_3)_2$ precursor used in this process was 0.01 M, which was much lower than the typical concentration of 0.025 M reported in the literature.[8,22] This layer of nanowires was then coated with a SAM of OTS, which rendered the top surface of the nanowire arrays superhydrophobic (water contact angle of ~165°; Figure 2a inset). Prior to the growth of the second-layer wires, the substrate was treated by UVO. Controlling the UVO treatment time allowed only the SAM coating at the top ends of the wires to be removed while leaving most of the coating on the side walls of the wires. After this treatment, the water contact angle of the ZnO nanowire arrays was reduced to ~70°. The substrate was then placed into a chemical bath to grow the second-layer ZnO nanowires. Figure 2b shows an SEM image of a two-layer assembly of ZnO nanowire arrays, where an evident boundary between the two layers can be seen. A closer examination of the boundary (Figure 2c) indicated that the second-layer wires started their growth from the top ends of the first-layer wires and grew along the same orientation as the first-layer wires. The area density of the second-layer wires was slightly smaller than that for the first layer. This is because some first-layer wires were not long enough to reach the top surface of the array and thus could not be contacted by the aqueous solution. Therefore, they failed to serve as seeds for the growth of second-layer wires. The second-layer wires were slightly wider than the first-layer wires because the wires also grew laterally as they grew vertically, although at a much slower rate. The differences in the widths and densities of the wires in different layers led to the boundary between the adjacent layers that was visible under SEM. Such differences also suggested that the growth of the new-layer wires did not significantly change the morphology of the previous-layer wires, and therefore, widening and fusion of the previous-layer wires at their roots were effectively avoided during the growth of the new layer.

Apparently, the internal surface area of the multilayer assembly of nanowire arrays increases as more layers are added to the assembly by

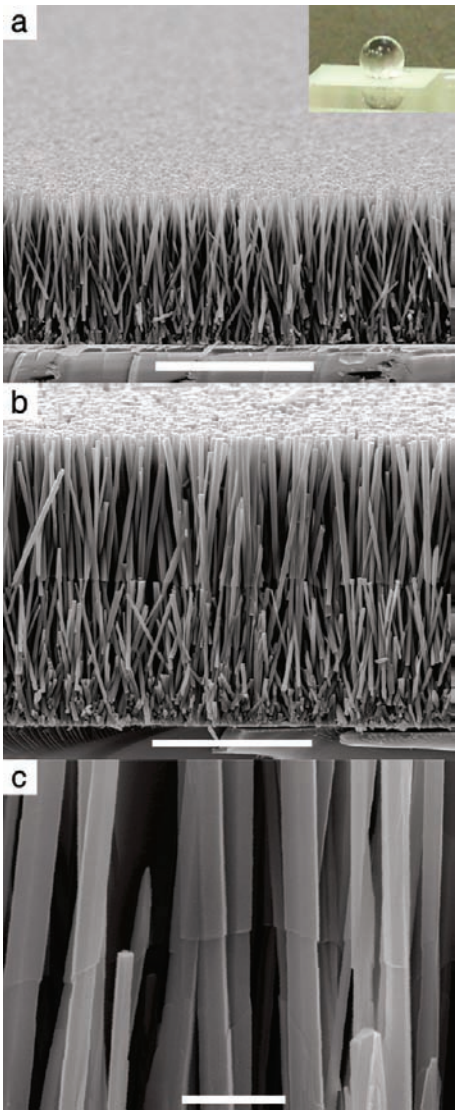

Figure 2. SEM images of the first and second layers of a ZnO nanowire array. (a) First-layer ZnO nanowire array. Inset: optical image of a water droplet on the array after it was coated with a SAM. Scale bar: 10 μm. (b) Two-layer assembly of ZnO nanowire arrays. Scale bar: 10 μm. (c) Junction between the first- and second-layer ZnO nanowires. Scale bar: 500 nm.

repeating this process. As a proof of concept, we made a four-layer assembly using this approach. Figure 3 shows an SEM image of this four-layer assembly of ZnO nanowire arrays, in which each layer was ~10 μm thick. The internal surface area is typically characterized by roughness factor (RF), which is defined as the ratio of the actual surface area to the projection area of the structure. Curve 1 in Figure 4 shows a plot of the RF of the four-layer assembly presented in Figure 3 as a function of the number of layers. It can be seen that the total RF of the four-layer array assembly was ~510, which is >5 times larger than what can possibly be obtained with a single-layer array. On the basis of curve 1, the RFs of the individual layers in the assembly (estimated as the increase in RF resulting from addition of the new layer to the assembly) are plotted as curve 2 in Figure 4. Curve 2 indicates that the RFs of the individual layers varied even though the thicknesses of the layers were the same. When the thickness is fixed, the RF of each layer is proportional to the product of the wire diameter and the wire density. For the same reason that

dx.doi.org/10.1021/ja202135n | J. Am. Chem. Soc. 2011, 133, 8122–8125

Figure 3. SEM image of a four-layer assembly of ZnO nanowire arrays. The thickness of each layer was ~10 μm. Scale bar: 10 μm.

the second-layer wires are wider and less dense than the first-layer wires, the width of the wires in each new layer is consistently larger than that of the previous layers, while concurrently the area density becomes smaller (Figure S1 in the Supporting Information). Therefore, the RF for each layer depends on the relative weighing of the two factors: the diameter and the area density of the wires. Curve 2 indicates that under our experimental conditions, the RF of the third layer was the largest, followed by the second and first layers, while the RF of the fourth layer was the smallest.

An intriguing question is whether there is a limit on the number of layers that can be assembled using this approach. Experiments showed that this assembly approach fails when the distance between the SAM-coated wires is too large to prevent aqueous solution from infiltrating into the wire arrays underneath the top layer. Top-view SEM images of the wires in different layers (Figure S1) show that as the number of layers increases, the area density of the wires decreases and the gap between adjacent wires becomes larger. The aqueous solution can enter the space between the wires if this gap becomes large enough that the capillary force generated between the hydrophobic side walls of the wires fails to overcome the hydrostatic pressure. Experimentally, we found that this happened when we tried to assemble more than 4−5 layers of wires using this approach. When the aqueous solution was able to infiltrate into the previously synthesized wire arrays, the wires underneath the new layer widened and even fused during the growth of the wires of the new layer.

The multilayer assembly of ZnO nanowire arrays provides an ideal electrode structure for DSCs. However, relative to TiO_2, ZnO has significant disadvantageous material properties when used as an anode material for DSCs, which may result in low values of the open-circuit voltage (V_{OC}) and fill factor (FF), leading to a low

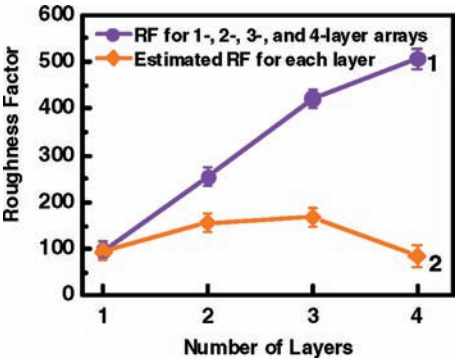

Figure 4. Roughness factor (RF) vs the number of layers for multiple-layer assemblies of ZnO nanowire arrays. Curve 1 shows the total RF as a function of the number of layers in the assembly. Curve 2 shows the RFs for the individual layers.

energy-conversion efficiency.[20] Therefore, for better characterization of DSCs based on such anode structures and to compare them with DSCs based on TiO_2 nanoparticles, we coated the ZnO nanowires with a 20−30 nm thick layer of TiO_2 (Figure S2) by a solution deposition method[20] before we sensitized the nanowire arrays and made final DSCs. Using this approach, we fabricated a series of DSCs from assemblies of one, two, three, and four layers of ZnO nanowire arrays. The thickness of each layer was kept at 10 μm, and the morphology of each layer may be represented by Figure 3.

The $I-V$ characteristics of these DSCs are presented in Figure 5a. As expected, the short-circuit current (I_{SC}), which largely depends upon the surface area of the arrays, increased almost linearly with the RF presented in Figure 4 as the total thickness of the assembly increased. The energy conversion efficiencies were 2.1, 4.6, 6.2, and 7.0%, respectively, for the DSCs made using one-, two-, three-, and four-layer assemblies of nanowire arrays. To our knowledge, the efficiency of 7.0% obtained for the four-layer, 40 μm thick assembly is the highest efficiency reported to date for this type of DSC. This efficiency is still lower than what has been reported for DSCs based on sintered nanoparticles, partly because the RF of the current four-layer assembly was only 510, which is smaller than the value of ~780 reported for sintered nanoparticle films.[23] However, it is believed that the RF of the multilayer assembly can be further increased by increasing the thickness of the array in each layer, and therefore, DSCs based on such multilayer assemblies may outperform the nanoparticle-based DSCs. Figure 5a also shows a slight decrease in V_{OC} and FF as the thickness of the multilayer array increased, possibly as a result of an increase in the series resistance of the DSCs. Figure 5b shows the incident-photon-to-current conversion efficiency (IPCE) versus wavelength for the DSCs fabricated using different numbers of array layers. As can be seen, increasing the total thickness of the multilayer assembly improved the IPCE at all wavelengths from 350 to 800 nm. An important feature observed in these IPCE curves is a significant red shift of the peak IPCE with increasing assembly thickness, indicating that the red-light absorption may be effectively improved by thickening the sensitized film with a vertically ordered structure. The consistently increasing IPCE, with a value of nearly 80% for the 40 μm thick assembly, also indicates that the electron collection by the multilayer arrays up to 40 μm thick is reasonably efficient. Relative to the increases in I_{SC} and IPCE upon addition of the second and third layers, growing the fourth layer brought a less significant increase in these parameters because the increase in RF (~70) as a result of adding the fourth layer wires was smaller than those (~150) for the second and third layers.

dx.doi.org/10.1021/ja202135n |J. Am. Chem. Soc. 2011, 133, 8122–8125

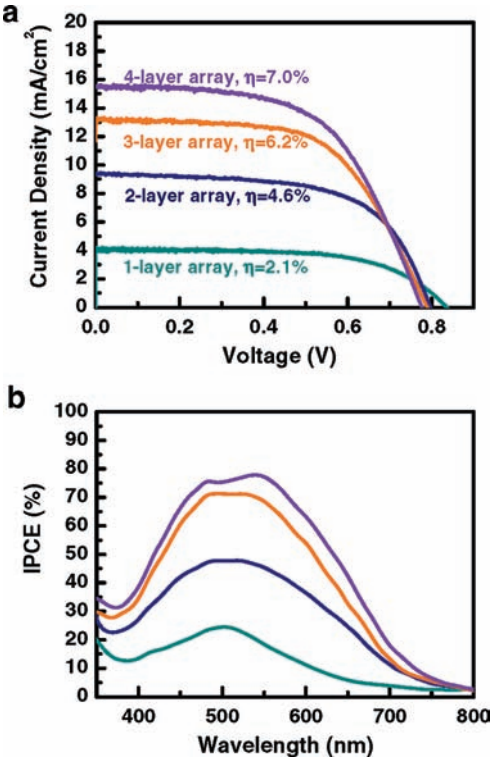

Figure 5. Photovoltaic performance of DSCs fabricated using the TiO_2-coated multilayer assemblies of ZnO nanowire arrays: (a) $I-V$ characteristics; (b) Plot of IPCE vs wavelength.

In addition to their application as an anode material for DSCs, ZnO nanowire arrays have been used in ultrasensitive chemical and biological sensors, organic solar cells, light-emitting diodes, nanogenerators, and nanopiezotronic devices.[24] It is hoped that the multilayer assemblies of ZnO nanowire arrays and the present approach for synthesizing such assemblies may find use in the development of these devices. Furthermore, ZnO nanowire arrays have been used as templates for fabricating TiO_2, Fe_2O_3, and CdSe nanotube arrays.[20,25,26] There is no apparent technical barrier to the use of these processes in fabricating multilayer TiO_2, Fe_2O_3, and CdSe nanotube arrays by employing the multilayer ZnO nanowire arrays as templates. Such vertically aligned structural materials with a high internal surface area may find applications in catalysis and as electrodes in batteries and fuel cells.[27,28]

In summary, we have developed a convenient approach for synthesizing multilayer assemblies of high-surface-area nanowire arrays. The approach involves alternate cycles of nanowire growth and self-assembled monolayer coating processes. As a demonstration, assemblies of one to four layers of ZnO nanowire arrays with a total thickness of up to 40 μm were synthesized. The internal surface area of the four-layer assembly was >5 times larger than what can possibly be obtained with a single-layer array. Such multilayer assemblies were used to fabricate DSCs with power conversion efficiencies of up to 7%. The potential of such an approach for synthesizing multilayers of vertically aligned nanowire arrays has not been fully explored, and it is believed that optimizing the process parameters and increasing the thickness of each layer will further increase the internal surface area of such assemblies, allowing DSCs with better performance to be fabricated.

■ ASSOCIATED CONTENT

Ⓢ Supporting Information. Experimental procedures, wire diameter and density data, and TEM images for TiO_2 coating. This material is available free of charge via the Internet at http://pubs.acs.org.

■ AUTHOR INFORMATION

Corresponding Author
gaod@pitt.edu

■ ACKNOWLEDGMENT

This work was supported by the National Science Foundation (Grant CBET 0967722).

■ REFERENCES

(1) Hardin, B. E.; Hoke, E. T.; Armstrong, P. B.; Yum, J.-H.; Comte, P.; Torres, T.; Fréchet, J. M. J.; Nazeeruddin, M. K.; Grätzel, M.; McGehee, M. D. *Nat. Photonics* **2009**, *3*, 406.
(2) Chen, C.-Y.; Wang, M.; Li, J.-Y.; Pootrakulchote, N.; Alibabaei, L.; Ngoc-le, C.-h.; Decoppet, J.-D.; Tsai, J.-H.; Grätzel, C.; Wu, C.-G.; Zakeeruddin, S. M.; Grätzel, M. *ACS Nano* **2009**, *3*, 3103.
(3) Feldt, S. M.; Gibson, E. A.; Gabrielsson, E.; Sun, L.; Boschloo, G.; Hagfeldt, A. *J. Am. Chem. Soc.* **2010**, *132*, 16714.
(4) Daeneke, T.; Kwon, T.-H.; Holmes, A. B.; Duffy, N. W.; Bach, U.; Spiccia, L. *Nat. Chem.* **2011**, *3*, 211.
(5) Tetreault, N.; Horvath, E.; Moehl, T.; Brillet, J.; Smajda, R.; Bungener, S.; Cai, N.; Wang, P.; Zakeeruddin, S. M.; Forro, L.; Magrez, A.; Grätzel, M. *ACS Nano* **2010**, *4*, 7644.
(6) Bai, Y.; Cao, Y.; Zhang, J.; Wang, M.; Li, R.; Wang, P.; Zakeeruddin, S. M.; Grätzel, M. *Nat. Mater.* **2008**, *7*, 626.
(7) Navas, J.; Guillen, E.; Alcantara, R.; Fernandez-Lorenzo, C.; Martin-Calleja, J.; Oskam, G.; Idigoras, J.; Berger, T.; Anta, J. A. *J. Phys. Chem. Lett.* **2011**, *2*, 1045.
(8) Law, M.; Greene, L. E.; Johnson, J. C.; Saykally, R.; Yang, P. D. *Nat. Mater.* **2005**, *4*, 455.
(9) Law, M.; Greene, L. E.; Radenovic, A.; Kuykendall, T.; Liphardt, J.; Yang, P. *J. Phys. Chem. B* **2006**, *110*, 22652.
(10) Fabregat-Santiago, F.; Bisquert, J.; Cevey, L.; Chen, P.; Wang, M.; Zakeeruddin, S. M.; Grätzel, M. *J. Am. Chem. Soc.* **2009**, *131*, 558.
(11) Snaith, H. J.; Humphry-Baker, R.; Chen, P.; Cesar, I.; Zakeeruddin, S. M.; Grätzel, M. *Nanotechnology* **2008**, *19*, No. 424003.
(12) Martinson, A. B. F.; Hamann, T. W.; Pellin, M. J.; Hupp, J. T. *Chem.—Eur. J.* **2008**, *14*, 4458.
(13) Galoppini, E.; Rochford, J.; Chen, H.; Saraf, G.; Lu, Y.; Hagfeldt, A.; Boschloo, G. *J. Phys. Chem. B* **2006**, *110*, 16159.
(14) Martinson, A. B. F.; McGarrah, J. E.; Parpia, M. O. K.; Hupp, J. T. *Phys. Chem. Chem. Phys.* **2006**, *8*, 4655.
(15) Martinson, A. B. F.; Goes, M. S.; Fabregat-Santiago, F.; Bisquert, J.; Pellin, M. J.; Hupp, J. T. *J. Phys. Chem. A* **2009**, *113*, 4015.
(16) Jennings, J. R.; Ghicov, A.; Peter, L. M.; Schmuki, P.; Walker, A. B. *J. Am. Chem. Soc.* **2008**, *130*, 13364.
(17) Mor, G. K.; Shankar, K.; Paulose, M.; Varghese, O. K.; Grimes, C. A. *Nano Lett.* **2006**, *6*, 215.
(18) Feng, X.; Shankar, K.; Varghese, O. K.; Paulose, M.; Latempa, T. J.; Grimes, C. A. *Nano Lett.* **2008**, *8*, 3781.
(19) Liu, B.; Aydil, E. S. *J. Am. Chem. Soc.* **2009**, *131*, 3985.
(20) Xu, C.; Shin, P.; Cao, L.; Wu, J.; Gao, D. *Chem. Mater.* **2010**, *22*, 143.
(21) Varghese, O. K.; Paulose, M.; Grimes, C. A. *Nat. Nanotechnol.* **2009**, *4*, 592.
(22) Xu, C.; Shin, P.; Cao, L.; Gao, D. *J. Phys. Chem. C* **2010**, *114*, 125.
(23) O'Regan, B.; Grätzel, M. *Nature* **1991**, *353*, 737.
(24) Wang, Z. L. *Mater. Sci. Eng., R* **2009**, *64*, 33.
(25) Liu, J.; Li, Y.; Fan, H.; Zhu, Z.; Jiang, J.; Ding, R.; Hu, Y.; Huang, X. *Chem. Mater.* **2010**, *22*, 212.
(26) Zhou, M.; Zhu, H.; Wang, X.; Xu, Y.; Tao, Y.; Hark, S.; Xiao, X.; Li, Q. *Chem. Mater.* **2010**, *22*, 64.
(27) Orera, A.; Slater, P. R. *Chem. Mater.* **2010**, *22*, 675.
(28) Ellis, B. L.; Lee, K. T.; Nazar, L. F. *Chem. Mater.* **2010**, *22*, 691.